JACS Au
AN OPEN ACCESS JOURNAL OF THE AMERICAN CHEMICAL SOCIETY

Open Access
This article is licensed under CC-BY 4.0

pubs.acs.org/jacsau
Article

At the "Peak" of Vis-to-UV Upconversion: Clear Advantages of TIPS Substituents for a Biphenyl Annihilator

Julian A. Moghtader, Masanori Uji, Till J. B. Zähringer, Matthias Schmitz, Luca M. Carrella, Alexander Heckel, Eva Rentschler, Nobuhiro Yanai,* and Christoph Kerzig*

Cite This: JACS Au 2025, 5, 5707−5716

Read Online

ACCESS | Metrics & More | Article Recommendations | Supporting Information

ABSTRACT: Sensitized triplet−triplet annihilation systems enable the efficient conversion of two low-energy photons from a low-intensity, noncoherent light source into one high-energy photon, opening avenues for diverse applications. The attachment of triisopropylsilylethynyl (TIPS-ethynyl) groups to aromatic compounds has led to the development of many annihilators with high upconversion quantum yields. Here, we synthesized a series of novel symmetrical biphenyls bearing silylethynyl substituents of varying sizes and evaluated them as annihilators in visible-to-UV upconversion systems. While all of these systems do not suffer from excimer formation issues, their upconversion performances differ significantly. Small substituents like trimethylsilylethynyl give similar upconversion quantum yields (up to ∼12%) as the TIPS-ethynyl groups, but the larger triphenylsilylethynyl substituents reduce the achievable quantum yields by half, which is likely due to additional nonradiative loss channels arising from altered energies of higher excited triplet states. The UV emission of the novel annihilators is hypsochromically shifted by about 20 nm relative to that of the TIPS-naphthalene benchmark UV annihilator, thereby reaching a highly attractive spectral region for bond activation photochemistry. Using the most efficient annihilator, bTIPS-BP, we achieved blue-to-UV upconversion-driven release of fluorescein from a photocage. In the greater context of photon upconversion and in view of other recent reports on substituent effects, our results indicate that several chromophore-specific effects must be understood for obtaining optimized systems.

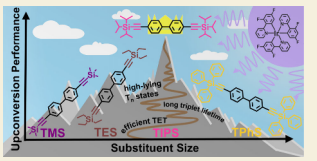

KEYWORDS: *Energy Transfer, Fluorescence Spectroscopy, Kinetics, Photochemistry, Time-Resolved Spectroscopy*

Downloaded via UNIV MAINZ on December 2, 2025 at 11:17:17 (UTC).
See https://pubs.acs.org/sharingguidelines for options on how to legitimately share published articles.

INTRODUCTION

Photon upconversion is a highly potent and versatile concept that can improve the performance of many contemporary technologies, such as photovoltaics, bioimaging, 3D printing, and various bond activation processes for chemical applications.[1−12] Many different strategies like two-photon absorption (2PA), lanthanide-based upconversion nanoparticles (UCNPs), nonlinear optics, or sensitized triplet−triplet annihilation upconversion (sTTA-UC) can be utilized for the absorption of two low-energy photons and their conversion into one high-energy photon.[13−17] Among these approaches, sTTA-UC shows great application potential since upconversion can operate under low incident excitation intensities utilizing noncoherent light sources.[18−21] Owing to the need for high-energy photons in a multitude of applications, blue-to-UV upconversion is an especially relevant topic.[17,22−26] The first blue-to-UV upconversion system via sensitized triplet−triplet annihilation upconversion was originally explored by Castellano et al. in 2006.[27] A system consisting of $Ir(ppy)_3$ as sensitizer (Sens) and 1,6-di-*tert*-butylpyrene as triplet energy acceptor and annihilator (An) was used, which laid the grounds for the implementation of blue-to-UV sTTA in chemical applications that would otherwise rely on high-energy UV excitation.[18,28−30] The interest in such upconversion systems received a further boost by the discovery of TIPS-naphthalene as a benchmark annihilator by Kimizuka and Yanai, which, in combination with the sensitizer $Ir(C6)_2(acac)$, yielded the first highly efficient blue-to-UV upconversion system with achievable quantum yields ϕ_{UC} beyond 10%.[31] With numerous recent application examples of blue-to-UV upconversion systems, such as in 3D printing, wastewater treatment, photocatalysis, and biomedical applications,[26,32−34] the interest in the development of novel, even more efficient vis-to-UV upconversion systems is still increasing.[35−41] Especially blue-to-UV upconversion systems generating wavelengths as short as possible are desired, where the high energy emission can photoexcite and activate a broad range of compounds and can overcome energy barriers that are inaccessible for visible-light driven systems.[42−44] A few upconversion systems that utilize sTTA-UC to generate photons in the UV-B or even the UV-C region have been developed (see Figure 1), but they lag behind in upconversion efficiency, leading to an enormous efficiency falloff for annihilators with emission wavelengths <365 nm. UV upconversion systems face challenges owing to the intrinsic nature of UV chemistry, such as quick degradation as well as

Received: September 12, 2025
Revised: October 23, 2025
Accepted: October 24, 2025
Published: November 7, 2025

© 2025 The Authors. Published by American Chemical Society

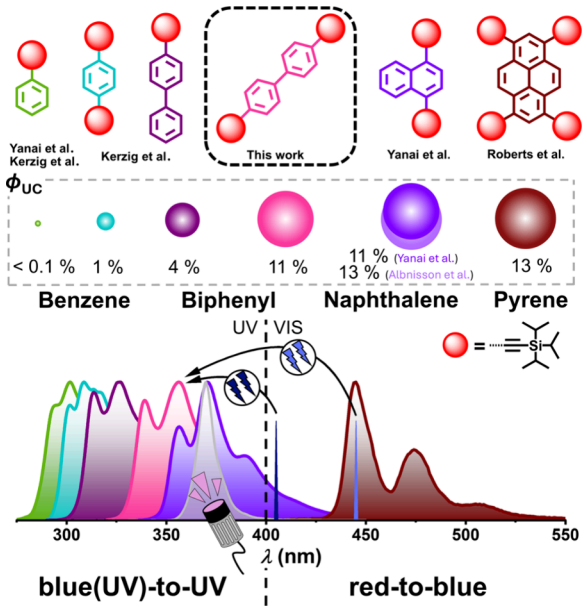

Figure 1. Emission spectra and external upconversion quantum yields ϕ_{UC} of TIPS-ethynyl (triisopropylsilylethynyl)-disubstituted biphenyl in comparison to already published annihilators used in upconversion systems that are based on TIPS-ethynyl modification (ϕ_{UC} is not corrected for filter effects; at infinite excitation intensities with a theoretical limit of 50%).[31,45,46,49,51−53] Vertical lines indicate the excitation wavelengths of the cw lasers used in this study. The gray spectrum was recorded for a 370 nm high-power LED; commercial high-power LEDs with significantly shorter emission wavelengths are not available. See the text for further explanations.

increased filter effects. Moreover, the high excited-state energies seem to be responsible for inherent loss channels during the TTA process that still have to be understood. However, this spectral range is highly attractive because commercial high-power LEDs with peak emission wavelengths <365 nm are not available.[45−49] This work extends the range of efficient upconversion (ϕ_{UC} > 10% in the linear region of the intensity dependence) systems to ∼350 nm in the UV region (emission onset at ∼325 nm, compare Figure 1), while simultaneously further exploring the influence of different substituents at the silylethynyl groups on potential annihilators.[50,51]

Recently, many studies have focused on the development of novel triplet annihilation chromophores, which revealed that the modification of an organic chromophore with **TIPS**-ethynyl (triisopropylsilylethynyl) groups is a viable pathway to synthesize novel annihilators with outstanding upconversion characteristics.[45,46,49,52,54−57] However, the exact role with all its advantages and disadvantages of this group is to this day only partially understood.[50,58−60] Owing to their high electron density, triisopropylsilylethynyl groups increase the singlet−triplet gap while expanding the amount of π-electrons minimally. This in turn increases the maximum achievable anti-Stokes shift for an upconversion system.[57,61−66] Additionally, the silyl substitution leads to improved fluorescence quantum yields ϕ_{Fl} for chromophores, thereby increasing the upconversion quantum efficiency of the respective upconversion system accordingly.[67,68] Albinsson et al. systematically substituted naphthalene at the 1,4 positions with different substituents at the silylethynyl moiety to explore the steric influence of methyl, isopropyl, and phenyl groups.[50] They concluded that bulkier substituents hamper excimer formation, leading to improved upconversion efficiencies. Interestingly, **TIPS**- and triphenylsilyl (**TPhS**)-ended ethynyl groups had essentially identical effects on the performance of the investigated mono- and disubstituted naphthalene annihilators. For trialkylsilylethynyl derivatives of pyrene, Roberts and co-workers showed that the smaller trimethylsilylethynyl (**TMS**-ethynyl) substituent leads to the most efficient upconversion, despite competitive excimer formation occurring.[51] While several structural modifications were tested to fine-tune bimolecular rate constants and the excited-state energies or to avoid excimer formation[69−71] for the frequently studied perylene annihilator chromophore in the past, the positive influence of **TIPS**-ethynyl groups was investigated only very recently.[50,51,57] On the other hand, recent results from Pun and co-workers suggest that some annihilator chromophores benefit from rather flat substituent "straps", which reduce the core-to-core distance and increase the spin-statistical *f* value of an annihilator.[72,73] Additional factors that could have an impact on the *f* value such as molecular orientation during the TTA process and minor effects on the excited-state energy landscape have barely been explored.[74−76]

As we will show, the effect of the different substituents at the silylethynyl groups is completely different for the novel biphenyl annihilator compared to what has been observed for pyrene and naphthalene derivatives. Specifically, the annihilator with two **TIPS**-ethynyl groups shows the most promising annihilator properties and outperforms the corresponding **TPhS** compound, which is explained by the different energies of higher-lying triplet states promoting loss channels in the **TPhS** derivative. We additionally exploit the excellent performance of the most efficient annihilator for a blue-light-driven uncaging reaction of **fluorescein**, which would otherwise require UV light.

RESULTS AND DISCUSSION

As the organic annihilator chromophore, we have chosen biphenyl and doubly substituted the core structure with four different silylethynyl groups, namely trimethylsilylethynyl (**TMS**), triethylsilylethynyl (**TES**), triisopropylsilylethynyl (**TIPS**), and triphenylsilylethynyl (**TPhS**) to yield the respective bis(trialkyl/phenyl)silylethynyl-biphenyl (**bTXS-BP**, Figure 2A). The novel annihilator compounds were prepared by Sonogashira coupling reactions starting from 4,4′-dibromobiphenyl, and their identities and purities were analyzed by mass spectrometry and ^{1}H as well as ^{13}C NMR spectroscopy. All analytical data sets are shown in the Supporting Information (SI, section 4). For **bTPhS-BP**, a crystal structure could be obtained after vapor diffusion crystallization (SI, section 5).

Trialkylsilyl groups are generally known to enhance fluorescence quantum yields.[67] When compared to unsubstituted biphenyl and mono-TIPS-substituted biphenyl (TIPS-biphenyl), this holds true: Biphenyl emits 15% of its initially absorbed photons, while TIPS-biphenyl has a fluorescence quantum yield (ϕ_{Fl}) of 48% in nonpolar solvents.[52,77] Accordingly, all four **bTXS-BP** compounds show high fluorescence quantum yields of ∼90% in strongly diluted cyclohexane and toluene solutions with a short singlet state lifetime τ_{Fl} of ∼0.7 ns (Table 1).

When the four newly synthesized chromophores are compared to each other, only minor differences can be found. Not only is this true for the fluorescence properties and

https://doi.org/10.1021/jacsau.5c01202
JACS Au 2025, 5, 5707−5716

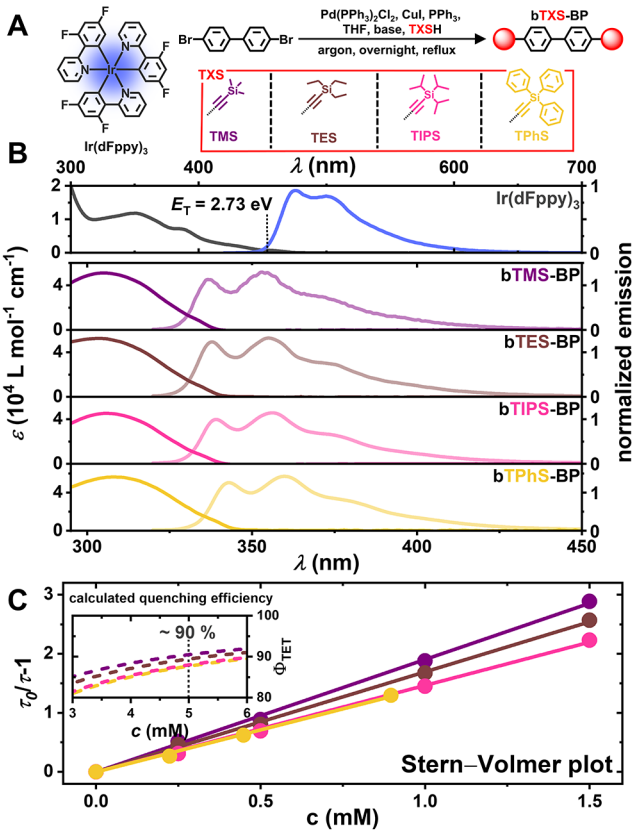

Figure 2. (A) Molecular structure of tris[3,5-difluoro-2-(2-pyridinyl)-phenyl]-iridium (**Ir(dFppy)$_3$**) and different biphenyl substituents **TXS** with the reaction scheme for the synthesis of the annihilators. (B) UV−vis absorption and normalized emission spectra of the sensitizer **Ir(dFppy)$_3$** and the annihilators (top to bottom): 4,4′-bis((trimethylsilyl)ethynyl)biphenyl (**bTMS-BP**, purple), 4,4′-bis-((triethylsilyl)ethynyl)biphenyl (**bTES-BP**, brown), 4,4′-bis-((triisopropylsilyl)ethynyl)biphenyl (**bTIPS-BP**, pink), and 4,4′-bis((triphenylsilyl)ethynyl)biphenyl (**bTPhS-BP**, yellow). (C) Stern−Volmer plot of ^{3}**Ir(dFppy)$_3$** quenching with different annihilator concentrations in toluene. The expected relative errors for the resulting quenching rate constants are below 5%. The inset shows the calculated quenching efficiency as a function of the annihilator concentration.

the energies of the lowest excited singlet state (S_1), but DFT calculations also predict that all four chromophores show similar properties with respect to their triplet states, as indicated by spin density and triplet energy calculations (SI, section 1.12). This was confirmed by 77 K measurements (see SI, Figure S13), which revealed a triplet energy of 2.31 eV for both **bTMS-BP** and **bTPhS-BP**, which is very similar to the calculated triplet energies (Table 1). UV−vis absorption spectroscopy showed that all chromophores have similar absorption bands with only **bTPhS-BP** being slightly red-shifted (Figure 2B). This makes all four compounds equally attractive to test them as annihilators for sTTA-UC.

Based on the above-mentioned annihilator properties, we have selected **Ir(dFppy)$_3$** as a sensitizer for our upconversion measurements. This complex still absorbs in the blue region of the visible spectrum while retaining a high triplet energy of 2.73 eV in toluene (Figure 2B), which would lay the grounds for a fast triplet energy transfer (TET) from **Ir(dFppy)$_3$** to the respective biphenyl derivative. Additionally, an efficient back-triplet energy transfer cannot proceed since ∼0.4 eV would be needed to undergo this endergonic process, whereas room temperature can only enable uphill energy transfer with energy differences of up to about 0.3 eV.[78−84] Choosing **Ir(dFppy)$_3$** might not be ideal for application-related usage, since reabsorption effects and a low molar absorption coefficient at the incident excitation wavelength (see Figure S19) reduce the achievable absolute upconversion quantum yield (ϕ_{UC}) and increase the upconversion threshold intensity (I_{th}). However, for comparative studies focusing on the inherent annihilator properties, our sensitizer choice is expected to be well-suited owing to its above-mentioned characteristics and high photostability. Stern−Volmer analyses were employed for all sensitizer−annihilator pairs, substantiating that the triplet energies of all four derivatives are close to each other. We observed merely a slight difference between the smallest biphenyl **bTMS-BP** and the largest quencher **bTPhS-BP**. While **bTMS-BP** quenches ^{3}**Ir(dFppy)$_3$** with a rate constant k_q = 1.35 × 10^9 M^{-1} s^{-1}, the quenching rate constant of **bTPhS-BP** was determined as k_q = 1.01 × 10^9 M^{-1} s^{-1} (Figure 2C). The difference in quenching rates can most likely be explained by the increased size and molecular weight that are introduced by the bulkier substituents: Compared to **bTPhS-BP**, **bTMS-BP** is significantly smaller (see also the comparative DFT-calculated structures in Figure S2), which leads to a higher diffusion rate through the solvent and therefore an improved rate for diffusion-based quenching. Steric hindrance and therefore limited accessibility of energy donor and acceptor orbitals are seemingly minor issues. At lower quencher concentrations, this discrepancy in the quenching rate can lead to similarly large differences in the quenching efficiency, but when an adequate quencher concentration is chosen, the difference shrinks to marginal values. For our selected standard conditions with 5 mM of the respective biphenyl derivative as quencher, this translates to a varying quenching efficiency

Table 1. Photophysical Properties of the Disubstituted Biphenyls

	bTMS-BP	bTES-BP	bTIPS-BP	bTPhS-BP
S_1 (eV)[a,b]	3.79	3.78	3.78	3.75
τ_{Fl} (ns)[a,c]	0.71	0.69	0.67	0.64
$\Phi_{Fl,\ 50\ \mu M}$ (%)[a,d]	90.1	90.5	90.8	90.1
T_1 (eV)[e]	2.31 (2.40)	− (2.46)	− (2.40)	2.31 (2.40)
$T_1 \rightarrow T_{n(Abs,max)}$ (nm)[a,f]	451	457	461	478

[a]Measured in toluene. [b]The excited singlet state energy is estimated by the intersection of the normalized absorption and emission spectra. [c]Measured using TCSPC, with a 293 nm EPLED as excitation source. [d]Determined by the absolute fluorescence quantum yield method using a concentration of 50 μM, see SI, Section 1.6. [e]Determined at the high-energy emission peak of the phosphorescence spectra measured in 2-methyl-tetrahydrofuran. Based on these measurements and the calculated triplet energy levels shown in parentheses, essentially identical triplet energies are expected for all derivatives. [f]Transient absorption maximum of the respective T_1 state using laser flash photolysis.

https://doi.org/10.1021/jacsau.5c01202
JACS Au 2025, 5, 5707−5716

between 90.5% (for **bTMS-BP**) and 87.7% (for **bTPhS-BP**, see Figure 2C, inset). This minor difference in the overall quenching efficiency should only influence the upconversion studies marginally.

We then turned to laser flash photolysis (LFP) measurements for analyzing the quenching mechanism of the reaction between ^{3}**Ir(dFppy)$_3$** and **bTXS-BP** and for identifying the quenching products. For this, we first compared the TA spectrum of ^{3}**Ir(dFppy)$_3$** after selective 355 nm excitation with transient absorption spectra in the presence of 3 mM **bTES-BP** as a representative quencher (Figure 3A). On the time scale of

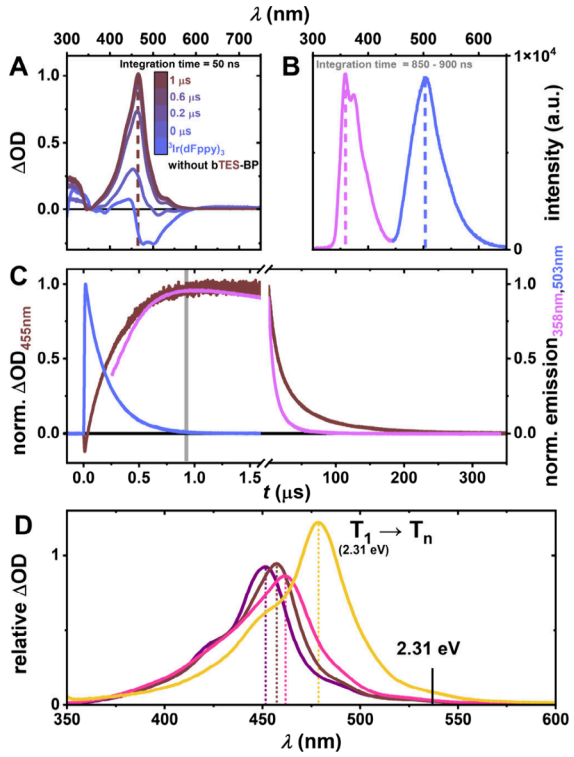

Figure 3. (A) Transient absorption (TA) spectra of a deaerated solution of 25 μM **Ir(dFppy)$_3$** and 3 mM **bTES-BP** in toluene at different delay times after laser excitation with 355 nm pulses (16 mJ, ~5 ns). For comparison, a TA spectrum of only 25 μM **Ir(dFppy)$_3$** in deaerated toluene is shown (light blue). (B) An emission spectrum of the same solution with a delay of 0.85 μs and time-integration over 50 ns is shown (detection window highlighted in panel C). (C) Normalized kinetic transient absorption (brown) and emission (blue, pink) decay traces of the same solution are shown. (D) TA spectra of 5 mM **bTMS-BP** (purple), **bTES-BP** (brown), **bTIPS-BP** (pink), and **bTPhS-BP** (yellow) in toluene with 30 μM **Ir(dFppy)$_3$** as sensitizer in deaerated toluene. The spectra were recorded 1 μs after excitation (100 ns integration), where emission of **Ir(dFppy)$_3$** was absent, indicating completion of the TET process. All other parameters such as laser intensity, detector settings, and probe lamp intensity were kept constant to yield spectra whose intensities reflect relative molar absorption coefficients.

1 μs, the transient absorption spectrum shifts from transient absorption signals that can be assigned to the triplet state of **Ir(dFppy)$_3$** with an apparent absorption maximum at 447 nm (due to emission contaminations in the TA spectrum), to the triplet state of **bTES-BP** with an absorption maximum at 457 nm.[45,52] A snapshot of the spectral emission after 0.85 μs additionally reveals that emission from both **Ir(dFppy)$_3$** and **bTES-BP** can be detected (Figure 3B). For **Ir(dFppy)$_3$**, this emission stems from the well-known room-temperature phosphorescence (which is not quenched completely in the given detection window). **bTES-BP** most likely exhibits delayed fluorescence resulting from sTTA-UC, given that the excited state singlet lifetime amounts to only ~0.7 ns for which no emission should be visible in that detection time window even if direct excitation would play a role. These results were confirmed by kinetic transient absorption and emission measurements at representative detection wavelengths (Figure 3C). Here, the phosphorescence emission of **Ir(dFppy)$_3$** decays with the same rate as the formation of ^{3}**bTES-BP**. The emission from ^{1}**bTES-BP*** rises and decays with a nonlinear dependence on the ^{3}**bTES-BP** concentration, a behavior that is typical for sTTA-UC processes.[85] While basic LFP experiments were performed with all biphenyl derivatives, more sophisticated concentration-dependent transient absorption measurements were carried out with **bTMS-BP** as the quencher and annihilator to find out whether excimer formation of the triplet state with a secondary molecule in the ground state can occur. Even at 20-times increased annihilator concentrations, no changes in the triplet state lifetime and the TA spectrum of the T_1 state could be detected during these measurements with standardized initial triplet concentrations (see SI, Figures S20 and S21).[50] Furthermore, the fluorescence quantum yield is only very slightly reduced when the **bTMS-BP** concentration increased from 50 μM to 5 mM from 90.1% to 87.7%. This minor change rules out excimer formation between a singlet-excited and a ground-state annihilator molecule and can be traced back to filter effects. Based on the absence of excimer formation for the sterically least hindered annihilator, we assume that excimer formation does not play any role for all annihilators of our study.[50,58] The transient absorption spectra of the biphenyl derivatives measured following TET show identical band structure, but their absorption maxima as well as their relative absorption coefficients vary (Figure 3D). On a photophysical basis, these observed triplet absorption bands can be assigned to $T_1 \rightarrow T_n$ transitions. The intensities of the absorption bands correlate with the electronic transition moments and the overlap integrals of the wave functions for nuclear vibrations of the T_1 states with their respective T_n states.[86] With an increasing substituent size, these transient absorption bands undergo a bathochromic shift from 451 nm for **bTMS-BP** to 478 nm for **bTPhS-BP**. Considering our aforementioned findings, this seems to be the only pronounced energetic difference between these different biphenyl derivatives.

For quantitative upconversion studies, the samples were prepared in an argon-filled glovebox to ensure identical conditions. To further substantiate the high (>85%) and very similar energy transfer quantum yields Φ_{TET} that we calculated with the Stern−Volmer equation (see above), measurements of the absolute quantum yield of the remaining (quenched) sensitizer emission were carried out. The resulting Φ_{TET} values (see Table 2) are very similar compared to the theoretical predictions shown in Figure 2C. In Figure 4A, the external (measured) upconversion quantum yield is plotted against the laser intensity (for raw data sets and selected upconversion spectra, see section 3.5 of the SI). Here, **bTIPS-BP** shows the highest experimentally measured upconversion quantum yield ($\phi_{UC,ext}$) of ~9.9%, with measured upconversion quantum yields of ~7.8%, ~7.3%, and ~2.8% for **bTMS-BP**, **bTES-BP**, and **bTPhS-BP**, respectively (with a maximum upconversion quantum yield of 50%).[87] In Figure 4B, the

https://doi.org/10.1021/jacsau.5c01202
JACS Au 2025, 5, 5707−5716

Table 2. Key Parameters of Upconversion Systems Consisting of 50 μM Ir(dFppy)$_3$ and 5 mM bTXS-BP in Toluene upon 405 nm cw Laser Excitation

	bTMS-BP	bTES-BP	bTIPS-BP	bTPhS-BP
$\Phi_{UC,ext}$ (%)	7.8	7.3	9.9	2.8
$\Phi_{UC,\infty}$ (%)[a]	11.8	11.4	11.4	5.5
I_{th} (W cm^{-2})[a]	12.5	15.0	2.7	33.5
$\Phi_{Fl,An}$ (%)	87.7	84.8	90.0	77.2
$\Phi_{Em,Sens}$ (%)	5.5	8.0	7.2	6.7
Φ_{TET} (%)[b]	92.8	89.6	90.6	91.3
f (%)[c]	20.2	21.5	20.4	11.7
$T_1 \rightarrow T_{n(Abs,2.31eV)}$[d]	1.0	1.0	1.3	3.6
τ_{An} (ms)[e]	0.67	0.45	1.47	0.49

[a]Estimated with experimental data as described by Murakami and Kamada.[85] [b]Determined by the residual emission $\Phi_{Em,Sens}$ of **Ir(dFppy)$_3$** in the sample. [c]This value represents the calculated lower limit of the f value, since it is only corrected for the reabsorption of the annihilator. For further details, see text and SI, Section 3.5. [d]Relative molar absorption coefficient of the $T_1 \rightarrow T_n$ transition at the energy of the T_1 state determined from the transient absorption spectra displayed in Figure 3 D; normalized to 1. See text for further explanations. [e]Determined utilizing TCSPC, see SI Section 1.8.

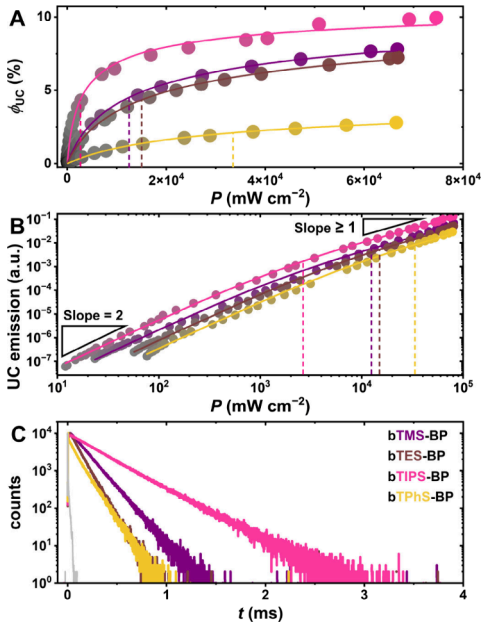

Figure 4. Triplet annihilation upconversion studies of deaerated solutions containing 50 μM **Ir(dFppy)$_3$** and 5 mM **bTXS-BP** in toluene using a 405 nm cw laser as an excitation source. (A) External quantum efficiency $\phi_{UC,\,ext}$ plotted against the excitation intensity. (B) Upconversion emission intensity plotted against the excitation intensity in a double logarithmic fashion. (C) Emission lifetime measurements of the upconversion emission, excited with a xenon flash lamp and equipped with a 445 nm band-pass filter and neutral density filters in the excitation beam. The sharp initial decrease in the lifetime curve for **bTPhS-BP** is a stray light artifact and does not affect the triplet lifetime determination.

upconversion emission is plotted against the laser intensity to reveal the threshold intensities I_{th} of the systems under study. Since only **bTIPS-BP** reaches a slope of 1 at high excitation intensities which would permit a simplified analysis, the I_{th} values of all samples were approximated using the fitting function developed by Murakami and Kamada.[85] This procedure revealed a threshold intensity of 2.7 W cm^{-2} for the system employing **bTIPS-BP**, while the other systems had threshold intensities exceeding 10 W cm^{-2} (see Table 2). In principle, a discrepancy in I_{th} values can be explained by the differences in triplet lifetimes *and* varying triplet−triplet annihilation rate constants of the individual triplet annihilators (see Figure S25 and related text for further explanations). The triplet lifetimes can be extracted from the upconversion emission lifetime at low excitation light intensities (Figure 4C). With an increased triplet lifetime, the threshold intensity is reduced (quadratically).[88] This behavior is qualitatively in good agreement with our measurements (Figure 4C), since **bTIPS-BP** shows the longest triplet excited state lifetime.

Since our upconversion measurement setup (see SI, section 1.5) did not allow us to increase the excitation intensity for all of our upconversion systems to reach their linear regime, we extrapolated our upconversion data to give us a theoretical external upconversion quantum yield maximum at an infinite excitation intensity ($\phi_{UC,\infty}$).[85] Here, the three compounds **bTMS-BP**, **bTES-BP**, and **bTIPS-BP** show nearly the same upconversion quantum yields at infinite excitation intensity $\phi_{UC,\infty}$ of 11.8%, 11.4%, and 11.4%, respectively. Only **bTPhS-BP** differs extensively with $\phi_{UC,\infty}$ = 5.5% (see Table 2). Utilizing these data sets, we estimated the spin statistical factor f. This was done with the following formula: $\phi_{UC,\infty} = 1/2 \times f \times \phi_{ISC} \times \phi_{TET} \times \phi_{TTA} \times \phi_{Fl}$.[72] Here, ϕ_{ISC} and ϕ_{TTA} are assumed to be unity, since **Ir(dFppy)$_3$** is known for a near-quantitative intersystem crossing quantum yield and an infinitely high excitation intensity leads to ϕ_{TTA} values close to unity as photophysical triplet deactivation cannot compete anymore.[89−91] We stress that the resulting f values have to be regarded as lower limits as we did not correct the upconversion quantum yields for optical losses mainly resulting from the reabsorption of the upconverted photons by the sensitizer (which strongly absorbs in the near UV region), from FRET, and from the usage of a 400 nm short-pass filter in our experimental setup (see Table S3 and related text for further explanations). However, we stress that these losses do not affect the comparability of the relative f values within our annihilator series. For **bTMS-BP**, **bTES-BP**, and **bTIPS-BP**, values of f = 20.2, 21.5, and 20.4% were found, respectively, while **bTPhS-BP** yielded f = 11.7%. An explanation for this discrepancy is provided by utilizing the differences in the observed $T_1 \rightarrow T_n$ absorption properties. A competitive process to the triplet annihilation $2 \times T_1 \rightarrow S_1$ is the nonradiative recombination to a higher triplet state $2 \times T_1 \rightarrow T_n$. This process is especially competitive when the energy difference from $2 \times T_1$ to T_n is small.[59,92] When comparing the transient absorption spectra (i.e., the absorption spectra of T_1) of the biphenyl derivatives, one can see that the triplet absorption spectrum of **bTPhS-BP** at the energy level of the excited triplet state (T_1 = 2.31 eV = 537 nm; corresponding to the transition to a T_n state at 4.62 eV) is more than twice as intense compared to all other compounds (see Figure 3 D), indicating a stronger transition moment for $T_1 \rightarrow T_n$ at that energy level. This directly translates into a more competitive $2 \times T_1 \rightarrow T_n$ loss pathway within the annihilation event and might explain the discrepancy in the spin statistical factor f between **bTPhS-BP** and all of the other biphenyl derivatives. The crystal structure that we obtained for **bTPhS-BP** revealed that two annihilator molecules can indeed accommodate a structure with the π-systems of two adjacent annihilator molecules in close proximity. The 7.4 Å distance between two aromatic core units (Figure S39, SI) should still enable

https://doi.org/10.1021/jacsau.5c01202
JACS Au 2025, 5, 5707−5716

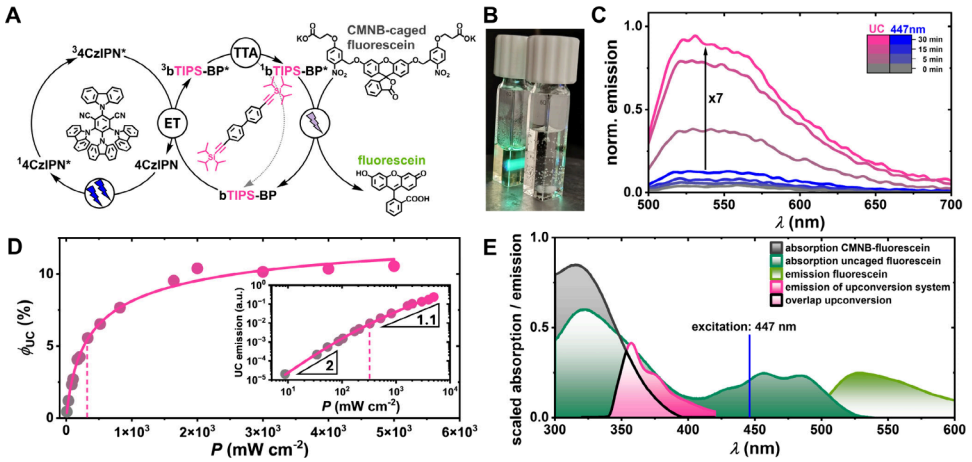

Figure 5. (A) Schematic representation of an sTTA-UC system (**4CzIPN** as sensitizer and **bTIPS-BP** as annihilator) used as a UV light source for the blue light-driven activation of **CMNB-caged fluorescein**. (B) Photograph of the uncaging setup with the upconversion solution consisting of 100 μM **4CzIPN** and 7 mM **bTIPS-BP** in argon-saturated toluene in the left cuvette excited with a blue (447 nm) cw laser and 15 μM **CMNB-caged fluorescein** in H_2O/DMF (1:1) in the right cuvette. (C) Emission from the cuvette with the uncaging reaction upon excitation at 490 nm after direct irradiation with a 447 nm cw laser (1 W, blue) or indirect irradiation as shown in panel B (pink). (D) External upconversion quantum yield plotted against the incident laser intensity. Inset: Double logarithmic plot of the upconversion emission versus the excitation power density. Measured with the setup described in ref 52. (E) Absorption spectra of **CMNB-caged fluorescein** (black), uncaged **fluorescein** (dark green) and emission spectra of **bTIPS-BP** in the upconversion system (pink) and of uncaged **fluorescein** (light green). The spectral overlap of the UC emission and the photocage absorption is highlighted with black borders.

productive annihilation considering that typical distances for the triplet pair on the order of 3−7 Å were reported for other annihilators.[41,72,88,93] Based on preliminary measurements, the triplet−triplet annihilation rate k_{TTA} seems to be slightly lower for **bTPhS-BP** compared to **bTIPS-BP** and much lower than that of **bTMS-BP**, either owing to the increased steric hindrance of the phenyl groups or as a result of slower diffusion (see SI, section 3.8). A more reliable analysis of all rate constants is difficult to achieve with our equipment. However, we believe that a recently developed technique with modulated cw diode lasers providing square-shaped pulses and simultaneous time-resolved emission detection is highly promising for the simultaneous determination of k_{TTA} and many other upconversion parameters in follow-up studies.[94] The reduced k_{TTA} value for **bTPhS-BP**, in conjunction with the even more drastically reduced triplet lifetime, negatively impacts the threshold intensity I_{th} and reduces application potential with low-intensity excitation sources. Based on our measurements, we conclude that **bTIPS-BP** shows the most beneficial properties as an annihilator for sTTA-UC. Since all biphenyl derivates suppress excimer formation in the singlet excited state and in the ground state, their achievable upconversion quantum yields can likely be ascribed to their excited state energy landscape. There, the **bTPhS-BP** annihilator suffers from lower lying triplet excited states T_n, which are more easily accessible as a competitive process to productive excited singlet generation from TTA, which inherently limits the upconversion efficiency of this compound to unexpectedly low levels when compared to the other biphenyl-based compounds.

Blue-to-UV upconversion allows the usage of lower energy emission wavelengths for applications that rely on higher energy excitation.[26] We demonstrate this by employing our most efficient annihilator (**bTIPS-BP**) with the broadly applied sensitizer (**4CzIPN**) to efficiently drive the uncaging reaction of **fluorescein** from its bis(5-carboxymethoxy-2-nitrobenzyl)ether fluorescein (**CMNB-caged fluorescein**).[95] Compared to **Ir(dFppy)$_3$**, **4CzIPN** absorbs more strongly in the blue spectral region and reabsorption of the upconverted emission is less pronounced (see Figure S19).[52] These beneficial properties should enable a lower threshold intensity, while facilitating applications with longer optical path lengths. The **CMNB-caged fluorescein** does not absorb light in the visible region. Upon the absorption of UV photons it cleaves off both (5-carboxymethoxy-2-nitrobenzyl) groups to yield the highly efficient green emitter **fluorescein** in solution.[96,97] The **fluorescein** release initiated by blue-to-UV upconversion can be detected by emission spectroscopy when exciting the sample in the blue/green region (490 nm in our case). When we directly irradiated a solution of 15 μM **CMNB-caged fluorescein** using a 447 nm cw laser at 1 W output power, almost no emission from the uncaged **fluorescein** could be detected, even after 30 min of irradiation. In contrast, by simply irradiating a degassed cuvette with our upconversion system, consisting of 100 μM **4CzIPN** and 7 mM **bTIPS-BP** (with the same 447 nm light source), next to the cuvette with **CMNB-caged fluorescein**, we were able to induce efficient release of **fluorescein** from its cage (Figure 5B,C). Here, the UC system is employed as light source for a radiative energy transfer (see ref 26 for the mechanistic diversity of UC-driven applications). Further control experiments with only degassed **4CzIPN** as a 447 nm illuminated system led to no conversion (compare Figure S12). Our blue-light-driven UC system thus serves as an effective UV light source: The upconverted emission following the sTTA process between **4CzIPN** and **bTIPS-BP** is reabsorbed by **CMNB-caged fluorescein**, which undergoes bond cleavage upon excitation (Figure 5A). Our blue light-driven system used for this application consisting of **4CzIPN** and **bTIPS-BP** has a high experimentally measured upconversion quantum yield $\phi_{UC,ext}$ of up to 10.5%, and the threshold intensity is relatively low with a value of 319 mW cm^{-2} (Figure 5D). Considering that the intersystem crossing quantum yield is reduced to ∼70% with **4CzIPN** in the solvent under study (toluene),[52] the lower limit of f for **bTIPS-BP**

https://doi.org/10.1021/jacsau.5c01202
JACS Au 2025, 5, 5707−5716

must be higher than that obtained with the iridium sensitizer (which gave a similar upconversion quantum yield despite an ISC quantum yield approaching unity), which is most likely due to reduced reabsorption effects.[52] Additionally, the longer-lived triplet state of **4CzIPN** leads to highly efficient triplet energy transfer (see SI, Figure S9), which further enhances the triplet energy transfer efficiency ϕ_{TET}. While the purely organic sensitizer clearly has some advantages over the Ir complex, its reduced photostability is a problem for long-term applications. Nevertheless, upconverted emission can still be detected after 30 min even with the highest excitation intensity of the most powerful cw laser used in this study (see SI, section 3.6). The absorption spectrum of **CMNB-caged fluorescein** overlaps in large parts with the upconverted emission spectrum of **bTIPS-BP**, which leads to a high percentage of photons that can be reabsorbed. We increased the concentration of **4CzIPN** in comparison to the upconversion quantum yield measurements to improve the absorption of 447 nm photons, while slightly reducing the upconversion efficiency.[98] These factors allow efficient uncaging despite a rather simple and nonoptimized setup with two cuvettes next to each other, in which about 92.5% of the upconverted photons do not hit the sample containing **CMNB-caged fluorescein** (see SI for details).[99]

CONCLUSIONS

In summary, we established a novel biphenyl-based annihilator for visible-to-UV upconversion and investigated the influence of differently sized substituents at the silylethynyl groups on the upconversion performance of the chromophore. We were able to confirm nearly identical photophysical properties for all four compounds, with the only major deviations found in the unquenched triplet lifetimes and the triplet−triplet absorption spectra, indicating that energetically lower $T_1 \rightarrow T_n$ transitions for the sterically larger phenyl substituents enable additional loss channels during the triplet annihilation event. With our novel molecular design, we were able to blue-shift the upconverted emission by about 20 nm compared to the TIPS-naphthalene benchmark compound,[31] thereby reaching a highly attractive spectral region in which commercial high-power UV-LEDs do not operate anymore. Simultaneously, a high experimentally measured upconversion quantum yield exceeding 10% could be maintained. Our novel annihilator molecule **bTIPS-BP** possesses the most attractive properties for blue-to-UV upconversion, and we exploited these properties through the combination with **4CzIPN** as sensitizer to activate **CMNB-caged fluorescein** in a simple emission-reabsorption setup. With this, we not only demonstrate the beneficial effects of the **TIPS**-group on the properties of an annihilator but also give additional insights into possible limitations of differently substituted silylethynyl groups. In contrast to recent studies with annihilators based on naphthalene and pyrene, excimer issues do not play any role, even with small methyl groups. What is more, long unquenched triplet lifetimes and the energy landscape of higher triplet states are responsible for the unique performance of the novel **bTIPS-BP** annihilator. Our studies also highlight the challenges associated with the identification of an ideal sensitizer for a novel UV annihilator as several factors such as filter effects and photostability must be considered. We hope that our work will contribute to the development of novel and even more efficient upconversion systems for future applications.

ASSOCIATED CONTENT

Data Availability Statement

All experimental data have been provided in the main text and the SI. The data sets shown in the main paper and DFT output files can be found under https://doi.org/10.25358/openscience-13600.

Supporting Information

The Supporting Information is available free of charge at https://pubs.acs.org/doi/10.1021/jacsau.5c01202.

Experimental details, analytical data, additional steady-state and time-resolved spectroscopic results, single crystal X-ray data and details about the irradiation experiment (PDF)

Accession Codes

Deposition Number 2464155 contains the supplementary crystallographic data for this paper. These data can be obtained free of charge via the joint Cambridge Crystallographic Data Centre (CCDC) and Fachinformationszentrum Karlsruhe Access Structures service.

AUTHOR INFORMATION

Corresponding Authors

Nobuhiro Yanai − *Department of Chemistry, Graduate School of Science, The University of Tokyo, Tokyo 113-0033, Japan;* orcid.org/0000-0003-0297-6544; Email: yanai@chem.s.u-tokyo.ac.jp

Christoph Kerzig − *Department of Chemistry, Johannes Gutenberg University Mainz, 55128 Mainz, Germany;* orcid.org/0000-0002-1026-1146; Email: ckerzig@uni-mainz.de

Authors

Julian A. Moghtader − *Department of Chemistry, Johannes Gutenberg University Mainz, 55128 Mainz, Germany;* orcid.org/0009-0005-3942-3021

Masanori Uji − *Department of Chemistry, Graduate School of Science, The University of Tokyo, Tokyo 113-0033, Japan;* orcid.org/0009-0001-6521-9236

Till J. B. Zähringer − *Department of Chemistry, Johannes Gutenberg University Mainz, 55128 Mainz, Germany;* orcid.org/0000-0001-9285-3980

Matthias Schmitz − *Department of Chemistry, Johannes Gutenberg University Mainz, 55128 Mainz, Germany;* orcid.org/0000-0003-0246-3036

Luca M. Carrella − *Department of Chemistry, Johannes Gutenberg University Mainz, 55128 Mainz, Germany;* orcid.org/0000-0001-9828-2912

Alexander Heckel − *Institute for Organic Chemistry and Chemical Biology, Goethe University Frankfurt, 60438 Frankfurt am Main, Germany*

Eva Rentschler − *Department of Chemistry, Johannes Gutenberg University Mainz, 55128 Mainz, Germany;* orcid.org/0000-0003-1431-3641

Complete contact information is available at: https://pubs.acs.org/10.1021/jacsau.5c01202

Funding

We acknowledge generous financial support from the JGU Mainz and the University of Tokyo. This work was supported by the Max Planck Graduate Center with the Johannes

Gutenberg-Universität Mainz (MPGC) and by the German Research Foundation (DFG, grant number KE 2313/3-1). This work was partly supported by the JST START (JPMJSF2303), JSPS KAKENHI (JP23KJ1717, JP23H00304), and The ANRI Fellowship.

Notes

The authors declare no competing financial interest.

■ ACKNOWLEDGMENTS

We thank Dr. Mihail Mondeshki for recording the mass spectra. J. A. M. is grateful for the support of the **Max Planck Graduate Center.** Parts of this research were carried out with the Elwetritsch supercomputer and the advisory services of the University of Kaiserslautern-Landau (https://hpc.rz.rptu.de), which is a member of the AHRP and the Gauss Alliance e.V.

■ REFERENCES

(1) Yuan, H.; Sun, K.; Su, X.; Hu, D.; Luo, Y.; Sun, Y.; Liu, Q.; Chen, L.; Qiao, J.; Xu, M.; Li, F. A Dark-State-Dominated Photochemical Upconversion Afterglow via Triplet Energy Transfer Relay. *Sci. Adv.* **2025**, *11* (17), No. eadt1225.

(2) Ji, H.; Luo, Z.; Yang, X.; Jin, X.; Zhao, T.; Duan, P. Chiral Dual-Annihilator Model for Controllable Photon Upconversion and Multi-Dimensional Optical Modulation. *Nat. Commun.* **2025**, *16* (1), 4952.

(3) Qi, F.; Feng, H.; Li, J.; Peng, Y.; Jiang, L.; Li, Y.; Zeng, L.; Huang, L. Amino Acids-Enabled Fast-Restore of Triplet-Triplet Annihilation Upconversion Luminescence for Background-Free Sensing of Herbicides. *Small Methods* **2025**, *9*, 2401945.

(4) Bharmoria, P.; Bildirir, H.; Moth-Poulsen, K. Triplet-Triplet Annihilation Based near Infrared to Visible Molecular Photon Upconversion. *Chem. Soc. Rev.* **2020**, *49* (18), 6529−6554.

(5) Chen, J.; Zhang, W.; Pullerits, T. Two-Photon Absorption in Halide Perovskites and Their Applications. *Mater. Horiz.* **2022**, *9* (9), 2255−2287.

(6) Wang, X.; Ding, F.; Jia, T.; Li, F.; Ding, X.; Deng, R.; Lin, K.; Yang, Y.; Wu, W.; Xia, D.; Chen, G. Molecular Near-Infrared Triplet-Triplet Annihilation Upconversion with Eigen Oxygen Immunity. *Nat. Commun.* **2024**, *15* (1), 2157.

(7) Luo, R.; Zhang, C.; Zhang, Z.; Ren, P.; Xu, Z.; Liu, Y. NIR-II Upconversion Nanomaterials for Biomedical Applications. *Nanoscale* **2025**, *17* (6), 2985−3002.

(8) Liang, G.; Wang, H.; Shi, H.; Wang, H.; Zhu, M.; Jing, A.; Li, J.; Li, G. Recent Progress in the Development of Upconversion Nanomaterials in Bioimaging and Disease Treatment. *J. Nanobiotechnology* **2020**, *18* (1), 154.

(9) Mettenbrink, E. M.; Yang, W.; Wilhelm, S. Bioimaging with Upconversion Nanoparticles. *Adv. Photonics Res.* **2022**, 3 (12), 2200098.

(10) Wang, Y.; Xu, W.; Liu, H.; Jing, Y.; Zhou, D.; Ji, Y.; Widengren, J.; Bai, X.; Song, H. A Multiband NIR Upconversion Core-Shell Design for Enhanced Light Harvesting of Silicon Solar Cells. *Light Sci. Appl.* **2024**, *13* (1), 312.

(11) Duan, J.; Liu, Y.; Zhang, Y.; Chen, Z.; Xu, X.; Ye, L.; Wang, Z.; Yang, Y.; Zhang, D.; Zhu, H. Efficient Solid-State Infrared-to-Visible Photon Upconversion on Atomically Thin Monolayer Semiconductors. *Sci. Adv.* **2022**, *8* (43), No. eabq4935.

(12) Richards, B. S.; Hudry, D.; Busko, D.; Turshatov, A.; Howard, I. A. Photon Upconversion for Photovoltaics and Photocatalysis: A Critical Review: Focus Review. *Chem. Rev.* **2021**, *121* (15), 9165−9195.

(13) Pawlicki, M.; Collins, H. A.; Denning, R. G.; Anderson, H. L. Two-Photon Absorption and the Design of Two-Photon Dyes. *Angew. Chem., Int. Ed.* **2009**, *48* (18), 3244−3266.

(14) Dong, H.; Sun, L.-D.; Yan, C.-H. Energy Transfer in Lanthanide Upconversion Studies for Extended Optical Applications. *Chem. Soc. Rev.* **2015**, *44* (6), 1608−1634.

(15) Medishetty, R.; Zaręba, J. K.; Mayer, D.; Samoć, M.; Fischer, R. A. Nonlinear Optical Properties, Upconversion and Lasing in Metal-Organic Frameworks. *Chem. Soc. Rev.* **2017**, *46* (16), 4976−5004.

(16) Zeng, L.; Huang, L.; Han, J.; Han, G. Enhancing Triplet-Triplet Annihilation Upconversion: From Molecular Design to Present Applications. *Acc. Chem. Res.* **2022**, *55* (18), 2604−2615.

(17) Förster, T.; Reifenberger, J.; Moumin, T.; Helmbold, J.; Antić, Ž.; Dramićanin, M. D.; Suta, M. Design Principles for (Efficient) Excited-State Absorption-Based Blue-to-UV Upconversion Phosphors with Pr^{3+}. *Chem. Sci.* **2025**, *16* (27), 12309−12323.

(18) Singh-Rachford, T. N.; Castellano, F. N. Photon Upconversion Based on Sensitized Triplet-Triplet Annihilation. *Coord. Chem. Rev.* **2010**, *254* (21−22), 2560−2573.

(19) Monguzzi, A.; Braga, D.; Gandini, M.; Holmberg, V. C.; Kim, D. K.; Sahu, A.; Norris, D. J.; Meinardi, F. Broadband Up-Conversion at Subsolar Irradiance: Triplet-Triplet Annihilation Boosted by Fluorescent Semiconductor Nanocrystals. *Nano Lett.* **2014**, *14* (11), 6644−6650.

(20) Gray, V.; Dzebo, D.; Abrahamsson, M.; Albinsson, B.; Moth-Poulsen, K. Triplet-Triplet Annihilation Photon-Upconversion: Towards Solar Energy Applications. *Phys. Chem. Chem. Phys.* **2014**, *16* (22), 10345−10352.

(21) Moghtader, J. A.; Bertrams, M.; Schollmeyer, D.; Kerzig, C. Mechanistic Insights: Correspondence on "Tuning Co-Operative Energy Transfer in Copper(I) Complexes Using Two-Photon Absorbing Diimine-Based Ligand Sensitizers.". *Angew. Chem., Int. Ed.* **2025**, *64*, No. e202509203.

(22) Chen, M.; Zhong, M.; Johnson, J. A. Light-Controlled Radical Polymerization: Mechanisms, Methods, and Applications. *Chem. Rev.* **2016**, *116* (17), 10167−10211.

(23) Matafonova, G.; Batoev, V. Recent Advances in Application of UV Light-Emitting Diodes for Degrading Organic Pollutants in Water through Advanced Oxidation Processes: A Review. *Water Res.* **2018**, *132*, 177−189.

(24) Goti, G.; Manal, K.; Sivaguru, J.; Dell'Amico, L. The Impact of UV Light on Synthetic Photochemistry and Photocatalysis. *Nat. Chem.* **2024**, *16* (5), 684−692.

(25) Raeiszadeh, M.; Adeli, B. A Critical Review on Ultraviolet Disinfection Systems against COVID-19 Outbreak: Applicability, Validation, and Safety Considerations. *ACS Photonics* **2020**, *7* (11), 2941−2951.

(26) Uji, M.; Zähringer, T. J. B.; Kerzig, C.; Yanai, N. Visible-to-UV Photon Upconversion: Recent Progress in New Materials and Applications. *Angew. Chem., Int. Ed.* **2023**, *62* (25), No. e202301506.

(27) Zhao, W.; Castellano, F. N. Upconverted Emission from Pyrene and Di- *Tert* -Butylpyrene Using $Ir(Ppy)_3$ as Triplet Sensitizer. *J. Phys. Chem. A* **2006**, *110* (40), 11440−11445.

(28) Singh-Rachford, T. N.; Castellano, F. N. Low Power Visible-to-UV Upconversion. *J. Phys. Chem. A* **2009**, *113* (20), 5912−5917.

(29) Wong, J.; Wei, S.; Meir, R.; Sadaba, N.; Ballinger, N. A.; Harmon, E. K.; Gao, X.; Altin-Yavuzarslan, G.; Pozzo, L. D.; Campos, L. M.; Nelson, A. Triplet Fusion Upconversion for Photocuring 3D-Printed Particle-Reinforced Composite Networks. *Adv. Mater.* **2023**, *35* (11), 2207673.

(30) Liu, R.; Chen, H.; Li, Z.; Shi, F.; Liu, X. Extremely Deep Photopolymerization Using Upconversion Particles as Internal Lamps. *Polym. Chem.* **2016**, *7* (14), 2457−2463.

(31) Harada, N.; Sasaki, Y.; Hosoyamada, M.; Kimizuka, N.; Yanai, N. Discovery of Key TIPS-Naphthalene for Efficient Visible-to-UV Photon Upconversion under Sunlight and Room Light**. *Angew. Chem., Int. Ed.* **2021**, *60* (1), 142−147.

(32) Lin, W.; Wen, H.; Li, J.; Wang, J.; Feng, H.; Huang, Z.; Li, R.; Zeng, L.; Huang, L. Compact Molecular Conformation of Prodrugs Enhances Photocleaving Performance for Tumor Vascular Growth Inhibition. *Adv. Healthc. Mater.* **2025**, *14* (1), 2402690.

(33) Peng, Y.; Li, J.-Y.; Qi, F.; Guo, D.-X.; Li, Y.-Z.; Feng, H.-J.; Jiang, L.-H.; Zhang, M.-Y.; Liu, Y.-X.; Zeng, L.; Huang, L. Highly Effective Near-Infrared to Blue Triplet-Triplet Annihilation Upcon-

https://doi.org/10.1021/jacsau.5c01202
JACS Au 2025, 5, 5707−5716

version Nanoparticles for Reversible Photobiocatalysis. *Nano Lett.* **2025**, *25* (13), 5291−5298.
(34) Feng, H.-J.; Zhang, M.-Y.; Jiang, L.-H.; Huang, L.; Pang, D.-W. Triplet-Triplet Annihilation Upconversion: From Molecules to Materials. *Acc. Chem. Res.* **2025**, DOI: 10.1021/acs.accounts.5c00403.
(35) Sanders, S. N.; Schloemer, T. H.; Gangishetty, M. K.; Anderson, D.; Seitz, M.; Gallegos, A. O.; Stokes, R. C.; Congreve, D. N. Triplet Fusion Upconversion Nanocapsules for Volumetric 3D Printing. *Nature* **2022**, *604* (7906), 474−478.
(36) O'Dea, C. J.; Isokuortti, J.; Comer, E. E.; Roberts, S. T.; Page, Z. A. Triplet Upconversion under Ambient Conditions Enables Digital Light Processing 3D Printing. *ACS Cent. Sci.* **2024**, *10* (2), 272−282.
(37) Huang, L.; Zeng, L.; Chen, Y.; Yu, N.; Wang, L.; Huang, K.; Zhao, Y.; Han, G. Long Wavelength Single Photon like Driven Photolysis via Triplet Triplet Annihilation. *Nat. Commun.* **2021**, *12* (1), 122.
(38) Uji, M.; Kondo, J.; Hara-Miyauchi, C.; Akimoto, S.; Haruki, R.; Sasaki, Y.; Kimizuka, N.; Ajioka, I.; Yanai, N. In Vivo Optogenetics Based on Heavy Metal-Free Photon Upconversion Nanoparticles. *Adv. Mater.* **2024**, *36*, 2405509.
(39) Barawi, M.; Fresno, F.; Pérez-Ruiz, R.; De La Peña O'Shea, V. A. Photoelectrochemical Hydrogen Evolution Driven by Visible-to-Ultraviolet Photon Upconversion. *ACS Appl. Energy Mater.* **2019**, *2* (1), 207−211.
(40) Pfund, B.; Steffen, D. M.; Schreier, M. R.; Bertrams, M.-S.; Ye, C.; Börjesson, K.; Wenger, O. S.; Kerzig, C. UV Light Generation and Challenging Photoreactions Enabled by Upconversion in Water. *J. Am. Chem. Soc.* **2020**, *142* (23), 10468−10476.
(41) Harada, N.; Shoyama, H.; Boonmong, N.; Mizukami, K.; Watanabe, Y.; Zhao, P.; Ehara, M.; Sasaki, Y.; Kimizuka, N. Sterically Protected π-Electron Systems Enable Efficient, Sunlight-Driven Solid-State Photon Upconversion. *ChemRxiv* **2025**, DOI: 10.26434/chemrxiv-2025-mmh9d-v2.
(42) Bintsis, T.; Litopoulou-Tzanetaki, E.; Robinson, R. K. Existing and Potential Applications of Ultraviolet Light in the Food Industry - a Critical Review. *J. Sci. Food Agric.* **2000**, *80* (6), 637−645.
(43) Barhoumi, A.; Liu, Q.; Kohane, D. S. Ultraviolet Light-Mediated Drug Delivery: Principles, Applications, and Challenges. *J. Controlled Release* **2015**, *219*, 31−42.
(44) Zhao, D.; Liu, S.; Wu, Y.; Guan, T.; Sun, N.; Ren, B. Self-Healing UV Light-Curable Resins Containing Disulfide Group: Synthesis and Application in UV Coatings. *Prog. Org. Coat.* **2019**, *133*, 289−298.
(45) Zähringer, T. J. B.; Moghtader, J. A.; Bertrams, M.; Roy, B.; Uji, M.; Yanai, N.; Kerzig, C. Blue-to-UVB Upconversion, Solvent Sensitization and Challenging Bond Activation Enabled by a Benzene-Based Annihilator. *Angew. Chem., Int. Ed.* **2023**, *62* (8), No. e202215340.
(46) Zähringer, T. J. B.; Heusel, C.; Schmitz, M.; Glorius, F.; Kerzig, C. Pushing the Limit of Triplet-Triplet Annihilation Photon Upconversion towards the UVC Range. *Chem. Commun.* **2025**, *61*, 9051.
(47) Hsu, T.-C.; Teng, Y.-T.; Yeh, Y.-W.; Fan, X.; Chu, K.-H.; Lin, S.-H.; Yeh, K.-K.; Lee, P.-T.; Lin, Y.; Chen, Z.; Wu, T.; Kuo, H.-C. Perspectives on UVC LED: Its Progress and Application. *Photonics* **2021**, *8* (6), 196.
(48) Hirayama, H.; Fujikawa, S.; Kamata, N. Recent Progress in AlGaN-Based Deep-UV LEDs. *Electron. Commun. Jpn.* **2015**, *98* (5), 1−8.
(49) Uji, M.; Nakagawa, S.; Nihonyanagi, A.; Miyajima, D.; Aizawa, N.; Yanai, N. Triplet-Triplet Annihilation Photon Upconversion Toward UVC Energy Generation Using TIPS-Benzene and a Heptazine Derivative. *Adv. Opt. Mater.* **2025**, *13*, No. e01279.
(50) Olesund, A.; Ghasemi, S.; Moth-Poulsen, K.; Albinsson, B. Bulky Substituents Promote Triplet-Triplet Annihilation Over Triplet Excimer Formation in Naphthalene Derivatives. *J. Am. Chem. Soc.* **2023**, *145* (40), 22168−22175.
(51) Isokuortti, J.; O'Dea, C. J.; Allen, S. R.; Vasylevskyi, S.; Page, Z. A.; Roberts, S. T. Putting the "P" Back in Delayed Fluorescence - Silylethynyl Substitution Generates Efficient Pyrene Annihilators for Red-to-Blue Photon Upconversion. *Adv. Opt. Mater.* **2025**, *13*, 2500388.
(52) Zähringer, T. J. B.; Bertrams, M.-S.; Kerzig, C. Purely Organic Vis-to-UV Upconversion with an Excited Annihilator Singlet beyond 4 eV. *J. Mater. Chem. C* **2022**, *10* (12), 4568−4573.
(53) Olesund, A.; Johnsson, J.; Edhborg, F.; Ghasemi, S.; Moth-Poulsen, K.; Albinsson, B. Approaching the Spin-Statistical Limit in Visible-to-Ultraviolet Photon Upconversion. *J. Am. Chem. Soc.* **2022**, *144* (8), 3706−3716.
(54) Wei, Y.; Pan, K.; Cao, X.; Li, Y.; Zhou, X.; Yang, C. Multiple Resonance Thermally Activated Delayed Fluorescence Sensitizers Enable Green-to-Ultraviolet Photon Upconversion: Application in Photochemical Transformations. *CCS Chem.* **2022**, *4* (12), 3852−3863.
(55) Nishimura, N.; Gray, V.; Allardice, J. R.; Zhang, Z.; Pershin, A.; Beljonne, D.; Rao, A. Photon Upconversion from Near-Infrared to Blue Light with TIPS-Anthracene as an Efficient Triplet-Triplet Annihilator. *ACS Mater. Lett.* **2019**, *1* (6), 660−664.
(56) Gilligan, A. T.; Owens, R.; Miller, E. G.; Pompetti, N. F.; Damrauer, N. H. Enhancing NIR-to-Visible Upconversion in a Rigidly Coupled Tetracene Dimer: Approaching Statistical Limits for Triplet-Triplet Annihilation Using Intramolecular Multiexciton States. *Chem. Sci.* **2024**, *15* (4), 1283−1296.
(57) Naimovicius, L.; Dapkevičius, M.; Radiunas, E.; Miroshnichenko, M.; Kreiza, G.; Alcaide, C.; Baronas, P.; Sasaki, Y.; Yanai, N.; Kimizuka, N.; Pun, A. B.; Solà, M.; Bharmoria, P.; Kazlauskas, K.; Moth-Poulsen, K. Enhancing the Statistical Probability Factor in Triplet-Triplet Annihilation Photon Upconversion via TIPS Functionalization. *Chem. Sci.* **2025**, DOI: 10.1039/D5SC05248C.
(58) Ye, C.; Gray, V.; Mårtensson, J.; Börjesson, K. Annihilation Versus Excimer Formation by the Triplet Pair in Triplet-Triplet Annihilation Photon Upconversion. *J. Am. Chem. Soc.* **2019**, *141* (24), 9578−9584.
(59) Naimovičius, L.; Radiunas, E.; Dapkevičius, M.; Bharmoria, P.; Moth-Poulsen, K.; Kazlauskas, K. The Statistical Probability Factor in Triplet Mediated Photon Upconversion: A Case Study with Perylene. *J. Mater. Chem. C* **2023**, *11* (42), 14826−14832.
(60) Olesund, A.; Gray, V.; Mårtensson, J.; Albinsson, B. Diphenylanthracene Dimers for Triplet-Triplet Annihilation Photon Upconversion: Mechanistic Insights for Intramolecular Pathways and the Importance of Molecular Geometry. *J. Am. Chem. Soc.* **2021**, *143* (15), 5745−5754.
(61) Maeda, H.; Fujii, T.; Minamida, K.; Mizuno, K. Fluorescence Properties of 1-(Silylethynyl)Naphthalenes and 1,4-Bis(Silylethynyl)-Naphthalenes in Solutions, Thin Films and Solid States. *J. Photochem. Photobiol. Chem.* **2017**, *342*, 153−160.
(62) Zeng, W.; Zhong, C.; Bronstein, H.; Plasser, F. Understanding and Tuning Singlet-Triplet (S_1 -T_1) Energy Gaps in Planar Organic Chromophores. *Angew. Chem., Int. Ed.* **2025**, *64* (21), No. e202502485.
(63) Manna, B. Does Triplet-Triplet Annihilation Favor Excimer Formation? A Case Study of Upconverted Fluorescence Emission with Zinc(II) Octaethylporphyrin-Doped 9,10-Bis[(Trialkylsilyl)-Ethynyl]Anthracene Nanoaggregates. *J. Phys. Chem. C* **2025**, *129* (21), 9809−9818.
(64) Radiunas, E.; Naimovičius, L.; Baronas, P.; Jozeliūnaitė, A.; Orentas, E.; Kazlauskas, K. CN-Tuning: A Pathway to Suppress Singlet Fission and Amplify Triplet-Triplet Annihilation Upconversion in Rubrene. *Adv. Opt. Mater.* **2025**, *13* (12), 2403032.
(65) Wang, H.; Zhao, C.; Burešová, Z.; Bureš, F.; Liu, J. Cyano-Capped Molecules: Versatile Organic Materials. *J. Mater. Chem. A* **2023**, *11* (8), 3753−3770.
(66) Wang, Z.; Wu, M.; Cui, X.; Ge, F.; Xiao, P.; Li, M.; Fu, H. Triplet-Triplet Annihilation Upconversion with Large Anti-Stokes Shift. *ACS Nano* **2025**, *19* (28), 25596−25616.

(67) Maeda, H.; Suzuki, T.; Segi, M. Effects of Substituents in Silyl Groups on the Absorption, Fluorescence and Structural Properties of 1,3,6,8-Tetrasilylpyrenes. *Photochem. Photobiol. Sci.* **2018**, *17* (6), 781−792.
(68) Anthony, J. E. Functionalized Acenes and Heteroacenes for Organic Electronics. *Chem. Rev.* **2006**, *106* (12), 5028−5048.
(69) Ye, C.; Gray, V.; Kushwaha, K.; Kumar Singh, S.; Erhart, P.; Börjesson, K. Optimizing Photon Upconversion by Decoupling Excimer Formation and Triplet Triplet Annihilation. *Phys. Chem. Chem. Phys.* **2020**, *22* (3), 1715−1720.
(70) Zeng, L.; Huang, L.; Lin, W.; Jiang, L.-H.; Han, G. Red Light-Driven Electron Sacrificial Agents-Free Photoreduction of Inert Aryl Halides via Triplet-Triplet Annihilation. *Nat. Commun.* **2023**, *14* (1), 1102.
(71) Huang, L.; Wu, W.; Li, Y.; Huang, K.; Zeng, L.; Lin, W.; Han, G. Highly Effective Near-Infrared Activating Triplet-Triplet Annihilation Upconversion for Photoredox Catalysis. *J. Am. Chem. Soc.* **2020**, *142* (43), 18460−18470.
(72) Naimovičius, L.; Zhang, S. K.; Pun, A. B. Impact of Steric Effects on the Statistical Probability Factor in Triplet-Triplet Annihilation Upconversion. *J. Mater. Chem. C* **2024**, *12*, 18374.
(73) Lyons, A. J.; Naimovičius, L.; Zhang, S. K.; Pun, A. B. Optimizing Upconversion Quantum Yield via Structural Tuning of Dipyrrolonaphthyridinedione Annihilators. *Angew. Chem., Int. Ed.* **2024**, No. e202411003.
(74) Bossanyi, D. G.; Sasaki, Y.; Wang, S.; Chekulaev, D.; Kimizuka, N.; Yanai, N.; Clark, J. Spin Statistics for Triplet-Triplet Annihilation Upconversion: Exchange Coupling, Intermolecular Orientation, and Reverse Intersystem Crossing. *JACS Au* **2021**, *1* (12), 2188−2201.
(75) Mulyadi, C. H.; Uji, M.; Parmar, B.; Orihashi, K.; Yanai, N. Triplet-Triplet Annihilation-Based Photon Upconversion with a Macrocyclic Parallel Dimer. *Precis. Chem.* **2024**, *2* (10), 539−544.
(76) Gray, V.; Dreos, A.; Erhart, P.; Albinsson, B.; Moth-Poulsen, K.; Abrahamsson, M. Loss Channels in Triplet-Triplet Annihilation Photon Upconversion: Importance of Annihilator Singlet and Triplet Surface Shapes. *Phys. Chem. Chem. Phys.* **2017**, *19* (17), 10931−10939.
(77) Montalti, M.; Credi, A.; Prodi, L.; Gandolfi, M. T. *Handbook of Photochemistry*; CRC Press, 2006. DOI: 10.1201/9781420015195.
(78) Meroni, D.; Monguzzi, A.; Meinardi, F. Photon Upconversion in Multicomponent Systems: Role of Back Energy Transfer. *J. Chem. Phys.* **2020**, *153* (11), 114302.
(79) Kalpattu, A.; Falvey, D. E.; Fourkas, J. T. Identifying Efficiency-Loss Pathways in Triplet-Triplet Annihilation Upconversion Systems. *Phys. Chem. Chem. Phys.* **2025**, *27* (21), 11000−11016.
(80) Li, Z.; Lu, J.; Li, X. Recent Progress in Thermally Activated Delayed Fluorescence Photosensitizers for Photodynamic Therapy. *Chem. - Eur. J.* **2024**, *30* (40), No. e202401001.
(81) Dias, F. B.; Penfold, T. J.; Monkman, A. P. Photophysics of Thermally Activated Delayed Fluorescence Molecules. *Methods Appl. Fluoresc.* **2017**, *5* (1), 012001.
(82) Isokuortti, J.; Kuntze, K.; Virkki, M.; Ahmed, Z.; Vuorimaa-Laukkanen, E.; Filatov, M. A.; Turshatov, A.; Laaksonen, T.; Priimagi, A.; Durandin, N. A. Expanding Excitation Wavelengths for Azobenzene Photoswitching into the Near-Infrared Range *via* Endothermic Triplet Energy Transfer. *Chem. Sci.* **2021**, *12* (21), 7504−7509.
(83) Strieth-Kalthoff, F.; Henkel, C.; Teders, M.; Kahnt, A.; Knolle, W.; Gómez-Suárez, A.; Dirian, K.; Alex, W.; Bergander, K.; Daniliuc, C. G.; Abel, B.; Guldi, D. M.; Glorius, F. Discovery of Unforeseen Energy-Transfer-Based Transformations Using a Combined Screening Approach. *Chem.* **2019**, *5* (8), 2183−2194.
(84) Kalpattu, A.; Fourkas, J. T. The Mechanisms of Endothermic Triplet Energy Transfer in Photochemical Systems. *Chem. Phys. Rev.* **2025**, *6* (3), 031305.
(85) Murakami, Y.; Kamada, K. Kinetics of Photon Upconversion by Triplet-Triplet Annihilation: A Comprehensive Tutorial. *Phys. Chem. Chem. Phys.* **2021**, *23* (34), 18268−18282.
(86) Balzani, V.; Ceroni, P.; Juris, A. *Photochemistry and Photophysics: Concepts, Research, Applications*; Wiley-VCH: Weinheim, Germany, 2014.
(87) Zhou, Y.; Castellano, F. N.; Schmidt, T. W.; Hanson, K. On the Quantum Yield of Photon Upconversion via Triplet-Triplet Annihilation. *ACS Energy Lett.* **2020**, *5* (7), 2322−2326.
(88) Monguzzi, A.; Mezyk, J.; Scotognella, F.; Tubino, R.; Meinardi, F. Upconversion-Induced Fluorescence in Multicomponent Systems: Steady-State Excitation Power Threshold. *Phys. Rev. B* **2008**, *78* (19), 195112.
(89) Amouri, H. Luminescent Complexes of Platinum, Iridium, and Coinage Metals Containing *N* -Heterocyclic Carbene Ligands: Design, Structural Diversity, and Photophysical Properties. *Chem. Rev.* **2023**, *123* (1), 230−270.
(90) Bachilo, S. M.; Weisman, R. B. Determination of Triplet Quantum Yields from Triplet-Triplet Annihilation Fluorescence. *J. Phys. Chem. A* **2000**, *104* (33), 7711−7714.
(91) Cheng, Y. Y.; Fückel, B.; Khoury, T.; Clady, R. G. C. R.; Tayebjee, M. J. Y.; Ekins-Daukes, N. J.; Crossley, M. J.; Schmidt, T. W. Kinetic Analysis of Photochemical Upconversion by Triplet-Triplet Annihilation: Beyond Any Spin Statistical Limit. *J. Phys. Chem. Lett.* **2010**, *1* (12), 1795−1799.
(92) Liu, S.; Gou, T.; Song, X.; Hu, R.; Liu, H.; Li, X.; Jiang, X. Study on the Energy Level Limitations of Triplet-Triplet Annihilation Upconversion with Anthracene-Isomerized Dimers as Annihilators. *ChemPhysMater.* **2024**, *3* (2), 187−193.
(93) Baronas, P.; Kreiza, G.; Naimovičius, L.; Radiunas, E.; Kazlauskas, K.; Orentas, E.; Juršėnas, S. Sweet Spot of Intermolecular Coupling in Crystalline Rubrene: Intermolecular Separation to Minimize Singlet Fission and Retain Triplet-Triplet Annihilation. *J. Phys. Chem. C* **2022**, *126* (36), 15327−15335.
(94) Edhborg, F.; Olesund, A.; Albinsson, B. Best Practice in Determining Key Photophysical Parameters in Triplet-Triplet Annihilation Photon Upconversion. *Photochem. Photobiol. Sci.* **2022**, *21* (7), 1143−1158.
(95) Zhou, Q.; Wirtz, B. M.; Schloemer, T. H.; Burroughs, M. C.; Hu, M.; Narayanan, P.; Lyu, J.; Gallegos, A. O.; Layton, C.; Mai, D. J.; Congreve, D. N. Spatially Controlled UV Light Generation at Depth Using Upconversion Micelles. *Adv. Mater.* **2023**, *35* (46), 2301563.
(96) Hapuarachchi, S.; Premeau, S. P.; Aspinwall, C. A. High-Speed Capillary Zone Electrophoresis with Online Photolytic Optical Injection. *Anal. Chem.* **2006**, *78* (11), 3674−3680.
(97) Kobayashi, T.; Urano, Y.; Kamiya, M.; Ueno, T.; Kojima, H.; Nagano, T. Highly Activatable and Rapidly Releasable Caged Fluorescein Derivatives. *J. Am. Chem. Soc.* **2007**, *129* (21), 6696−6697.
(98) Baronas, P.; Lekavičius, J.; Majdecki, M.; Elholm, J. L.; Kazlauskas, K.; Gaweł, P.; Moth-Poulsen, K. Automated Research Platform for Development of Triplet-Triplet Annihilation Photon Upconversion Systems. *ACS Cent. Sci.* **2025**, *11* (3), 413−421.
(99) Larsson, W.; Morimoto, M.; Irie, M.; Andréasson, J.; Albinsson, B. Diarylethene Isomerization by Using Triplet-Triplet Annihilation Photon Upconversion. *Chem. - Eur. J.* **2023**, *29* (13), No. e202203651.

https://doi.org/10.1021/jacsau.5c01202
JACS Au 2025, 5, 5707−5716